Lake surface-sediment pollen dataset for the alpine meadow vegetation type from the eastern Tibetan Plateau and its potential in past climate reconstructions

Xianyong Cao[1,~~2~~]*, Fang ~~Tian[3]~~Tian[2], Kai ~~Li[4]~~Li[3], Jian ~~Ni[4]~~Ni[3], Xiaoshan Yu[1], Lina Liu[1], Nannan Wang[1]

[1] Alpine Paleoecology and Human Adaptation Group (ALPHA), State Key Laboratory of ~~Alpine Ecology,~~Tibetan Plateau Earth System, Resources and Environment (TPESRE), Institute of Tibetan Plateau Research, Chinese Academy of Sciences, Beijing 100101, China

~~[2] CAS Center for Excellence in Tibetan Plateau Earth Sciences, Institute of Tibetan Plateau Research, Chinese Academy of Sciences (CAS), Beijing 100101, China~~

~~[3] Beijing Key Laboratory of Resource Environment and GIS,~~ [2] College of Resource Environment and Tourism, Capital Normal University, Beijing, 100048, China

[~~4~~3] College of Chemistry and Life Sciences, Zhejiang Normal University, Jinhua, 321004, China

Correspondence: Xianyong Cao (xcao@itpcas.ac.cn)

Abstract

A modern pollen dataset with an even distribution of sites is essential for pollen-based past vegetation and climate estimations. As there were geographical gaps in previous datasets covering the central and eastern Tibetan Plateau, lake surface-sediment samples (n=117) were collected from the alpine meadow region on the Tibetan Plateau between elevations of 3720 and 5170 m a.s.l. Pollen identification and counting were based on standard approaches, and modern climate data were interpolated from a robust modern meteorological dataset. A series of numerical analyses revealed that precipitation is the main climatic determinant of pollen spatial distribution~~;~~: Cyperaceae, Ranunculaceae, Rosaceae, and *Salix* indicate wet climatic conditions, while Poaceae, *Artemisia*, and Chenopodiaceae represent drought. Model performance of both weighted-averaging partial least squares (WA-PLS) and the random forest (RF) algorithm suggest that this modern pollen dataset has good predictive power in estimating the past precipitation ~~for~~from pollen spectra from the eastern Tibetan Plateau. In addition, a comprehensive modern pollen dataset can be established by combining our modern pollen dataset with previous datasets, which will be essential for the reconstruction of vegetation and climatic signals for fossil pollen ~~sprecta~~spectra on the Tibetan Plateau. Pollen datasets including both pollen counts and percentages for each sample together with their site location and climatic data are available at the National Tibetan Plateau Data Center (TPDC; DOI: 10.11888/Paleoenv.tpdc.271191).

1 Introduction

The relationship between modern pollen and climate, and its representation of vegetation, is the basis for explaining and reconstructing past climate and vegetation qualitatively or quantitatively (Juggins and Birks, 2012), so improving the quality of the modern pollen dataset is a primary step for an objective investigation of the modern relationship and to ensure reliable climate and vegetation reconstructions (Cao et al., 2018). To make the pollen-source area and taphonomy as compatible as possible, modern pollen assemblages should be retrieved from the same type of sedimentary environment as the fossil pollen spectra (Birks et al., 2010). Hence, to reconstruct past climate and vegetation from fossil pollen extracted from a lacustrine sediment, a corresponding modern pollen dataset of samples collected from lake surface-sediments is necessary. Although there are some modern pollen datasets for the Tibetan Plateau, established to investigate the relationships between pollen and climate or vegetation (Shen et al., 2006; Herzschuh et al., 2010; Ma et al., 2017), there are geographical gaps (e.g. the central and eastern Tibetan Plateau) in the sampled lakes which may bias interpretations.

The available modern pollen datasets reveal that pollen assemblages on the Tibetan Plateau are generally simple with Cyperaceae, *Artemisia*, Poaceae, and Chenopodiaceae as the dominant taxa (e.g. Herzschuh et al., 2010; Cao et al., 2014), with arboreal pollen taxa becoming more influential in the marginal areas (e.g. Ma et al., 2017; Li et al., 2020). It is essential to identify the climatic indicators of the modern pollen taxa (particular for the four dominant taxa) on the Tibetan Plateau, because the climatic indicators derived from modern pollen datasets from the surrounding lowland cannot be directly employed on the Tibetan Plateau. With our current modern pollen dataset extracted from lake surface-sediments we aim to 1) fill a geographical gap and thus establish a comprehensive modern pollen dataset covering the entire Tibetan Plateau; 2) determine the climatic indicators for common pollen taxa from the alpine meadow ecosystem; and 3) evaluate the predictive power of the modern dataset to reconstruct past climate and assess the reliability of the random forest algorithm in calibrating the pollen-climate relationship.

2 Study area

The elevation range of the lakes sampled for our pollen dataset is between 3720 and 5170 m a.s.l. with a median of 4420 m a.s.l. (the 25% quantile is 4230 m a.s.l and the 75% quantile is 4550 m a.s.l.; Figure 1). Climate of this region is controlled by the Asian Summer Monsoon in summer with warm and wet climatic conditions, and by westerlies in winter with cold and dry conditions (Wang, 2006). The eastern and central Tibetan Plateau containing these sampled lakes (with >4000 m a.s.l elevation) is covered by alpine meadow with sporadic patches of subalpine shrub. The plant communities of the alpine meadow are dominated by *Kobresia* species (Cyperaceae) generally, with Ranunculaceae, Asteraceae, *Polygonum* (Polygonaceae), *Potentilla* (Rosaceae), Fabaceae, and Caryophyllaceae as the common taxa. The subalpine shrub is generally distributed on the northern slopes of mountains with *Salix oritrepha* and *Potentilla fruticosa* as the main shrub components, while the herbaceous taxa mentioned above are also common (Wu, 1995; Herzschuh et al., 2010; unpublished vegetation survey).

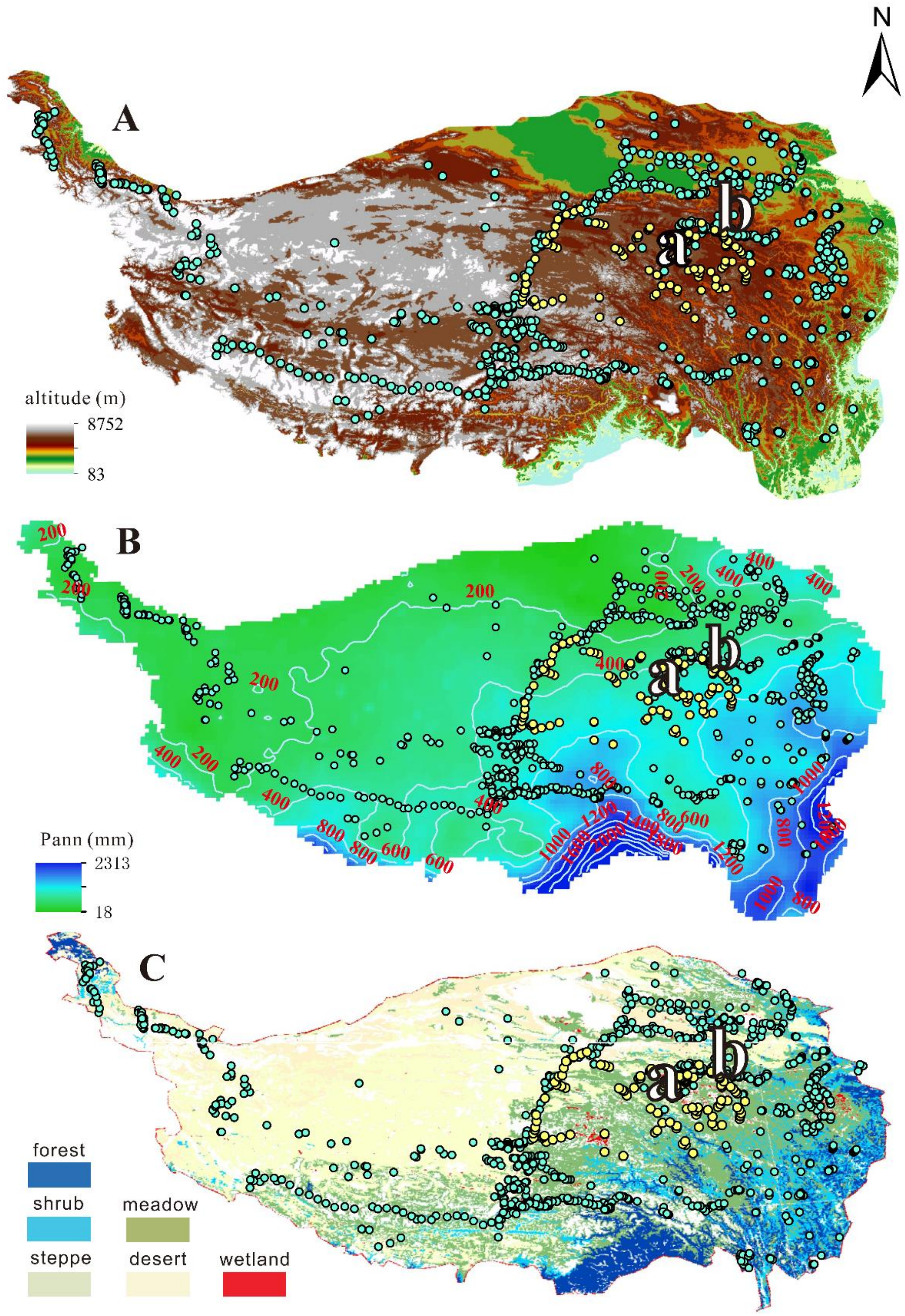

Figure 1 Spatial distribution of modern pollen samples (yellow dots: the 117 sampled lakes; bluish green dots: previous samples (surface-soils and lake surface-sediments)

included in the dataset of Cao et al., 2014). A: Digital Elevation Model; B: isohyet map (mm); C: vegetation map. “a” and “b” indicate the locations of Koucha Lake and Xingxinghai Lake.

3 Materials and methods

3.1 Sample collecting and pollen processing

To ensure the even distribution of the representative lakes, we travelled not only along the hardened roads but also the dirt roads to collect samples from the alpine meadow on the eastern and central Tibetan Plateau, in July and August 2018. ~~Generally~~To reduce the influence of long-distance pollen grains transported by wind and rivers, small and shallow ~~unnamed~~ lakes (or pools) with less than 100-m radius and without long inflow rivers (n=117) (locally sourced pollen grains are the dominant components for small lakes; Sugita, 1993) were selected to ~~reduce the influence of long-distance pollen transported by wind or rivers~~collect pollen samples (Figure 1). To reduce the influence of the ~~local~~lake-shore vegetation component~~ from the lake shore~~, the lake surface-sediment samples were collected from the central part of each lake, with the top 2 cm of lake sediment forming the sample~~.~~ (Tian et al., 2008). Although the selected lakes generally have an even distribution, there is still a gap in the south-west part of study area because of a lack of lake and road access (Figure 1).

For pollen extraction, approximately 10 g (wet untreated sediment) per sample were sub-sampled. Pollen samples were processed using standard acid-alkali-acid procedures (including 10% HCl, 10% KOH, 40% HF and 9:1 mixture of acetic anhydride and sulphuric acid successively~~,~~; Fægri and Iversen, 1975) followed by 7-μm-mesh sieving. A tablet with *Lycopodium* spores (27560 grains/tablet) was added to each sample prior to pollen extraction as tracers (Maher, 1981). Pollen grains were identified with the aid of modern pollen reference slides collected from the eastern and central Tibetan Plateau (including 401 common species of alpine meadow; Cao et al., 2020) and published atlases for pollen and spores (Wang et al., 1995; Tang et al., 2017).

More than 500 terrestrial pollen grains were counted for each sample, and more than 200 *Lycopodium* spores were counted for most of the samples (mean=270 grains; median=480 grains), both of which ensure a reliable representation of the entire pollen assemblage by the counted pollen data.

3.2 Data processing

To obtain modern climatic data for the sampled lakes, the Chinese Meteorological Forcing Dataset (CMFD; gridded near-surface meteorological dataset) with a temporal resolution of three hours and a spatial resolution of 0.1° was employed (He et al., 2020). The CMFD is made through the fusion of remote-sensing products, reanalysis datasets, and *in situ* station data between January 1979 and December 2018, and its high reliability has already ~~be~~been confirmed for western China including the Tibetan Plateau (He et al., 2020). Geographical distances of each sampled lake to each pixel in the CMFD were calculated based on their longitude/latitude coordinates using the *rdist.earth* function in the *fields* package version 9.6.1 (Nychka, et al., 2019) for R (version 3.6.0; R Core Team, 2019), and the ~~climatic data~~meteorological data (three-hour resolution between January 1979 and December 2018) of the nearest pixel to a sampled lake were assigned to represent the climatic conditions of that lake. Finally, the mean annual precipitation (P_{ann}; mm), mean annual temperature (T_{ann}; °C), and mean temperature of the coldest month (Mt_{co}; °C) and warmest month (Mt_{wa}; °C) were calculated for each sampled lake based on the long-term continuous meteorological data.

To visualize the relationships between modern pollen assemblages and climatic variables, ordination techniques were employed based on the square-root transformed pollen data of 19 taxa (those present in at least 3 samples and with a ≥ 3% maximum) to stabilize variances and optimize the signal-to-noise ratio (Prentice, 1980). Detrended correspondence analysis (DCA; Hill and Gauch, 1980) revealed that the length of the first axis of the pollen data was 1.44 SD (standard deviation units), indicating a linear response model is suitable for our pollen dataset (ter Braak and Verdonschot, 1995).

We performed redundancy analysis (RDA) to visualize the distribution of pollen species and sampling sites along the climatic gradients, selecting the minimal adequate model using forward selection and checking the variance inflation factors (VIF) at each step. If VIF values were higher than 20, which ~~indicate~~indicates that some variables in the model are co-linear, we stopped adding variables (ter Braak and Prentice, 1988). These ordinations were performed using the *decorana* and *rda* functions in the *vegan* package version 2.5-4 (Oksanen et al., 2019) for R.

Boosted regression tree (BRT) analysis was applied to determine how strongly the climatic variables influence the distribution of each individual pollen taxon, using square-root transformed pollen percentages. A BRT model was generated using the *gbm.step* function in the *dismo* package 1.0-12 version (Hijmans et al., 2015) for R with a Gaussian error distribution.

The basic assumption of pollen-based past climate reconstruction assumes that pollen taxa recorded in the modern calibration-set have similar ecological requirements as those in the fossil spectra (Juggins and Birks, 2012); in other words, the modern vegetation-climate relationship is assumed to be stable temporally through the target period for reconstruction. To evaluate the potential of the pollen dataset for past climate reconstruction, both the traditional method of weighted-averaging partial least squares (WA-PLS) and a new approach using the random forest (RF) algorithm were run. WA-PLS was performed using the *WAPLS* function in the *rioja* package version 0.7-3 (Juggins, 2012) for R using leave-one-out cross-validation, pollen percentages of the 19 selected pollen taxa were square-root transformed, and the number of WA-PLS components used was selected using a randomization *t*-test (Juggins and Birks, 2012). We performed the RF algorithm with the *randomForest* package (version 4.6-14; Liaw, 2018) in R. RF is an algorithm that integrates multiple decision trees, and the importance of each explanatory variable is measured as the percentage increase in the residual sum of squares after randomly shuffling the order of the variables to determine which explanatory variable can be added to the model. In our study, the importance of all pollen taxa on the spatial distribution of P_{ann} was estimated and the model systematically optimized by a stepwise reduction in variables by deleting the least important one. Our final RF model includes 19 pollen taxa (Appendix ~~2~~B), which all make a positive contribution to the precipitation distribution. To assess the predictive power of our pollen dataset, pollen spectra from Koucha Lake (covering the last 16 cal ka BP~~;~~ (calibrated thousand years before 1950 CE); 34.0°N; 97.2°E, 4540 m a.s.l.; Herzschuh et al., 2009~~; cal ka BP: calibrated thousand year before 1950 AD~~) and Xingxinghai Lake (covering the last 7.5 cal ka BP; 34.8°N, 98.1°E, 4228 m a.s.l.; Zhang et al., unpublished) were selected as the target fossil pollen datasets for quantitative reconstruction. A statistical significance test for all reconstructions was performed following the methods described in Telford and Birks (2011) using the *randomTF* function in the *palaeoSig* package version 1.1.2 for both WA-PLS and RF reconstruction methods separately (Telford, 2013).

3.~~3~~4 Data description

Pollen assemblages of the dataset from alpine ~~meadow~~meadows are dominated by Cyperaceae (mean 68.4%, maximum 95.9%), with other herbaceous pollen taxa common including Poaceae (mean 10.3%, maximum 87.7%), Ranunculaceae (mean 4.8%, maximum 33.6%), *Artemisia* (mean 3.7%, maximum 24.5%), and Asteraceae (mean 2.1%, maximum 33.6%). *Salix* (mean 0.4%, maximum 5.3%) is the major shrub taxon in these pollen assemblages, while arboreal taxa occur with low percentages generally (mean total arboreal percentage 0.9%, maximum 5.8%), mainly comprising *Pinus* (mean 0.3%, maximum 1.8%), *Betula* (mean 0.1%, maximum 0.9%), and *Alnus* (mean 0.1%, maximum 0.7%). ~~These~~Published vegetation data (e.g. Wu, 1995; Herzschuh et al., 2010) and our vegetation survey reveal that trees are absent from the alpine meadow communities within the study area, thus we believe the arboreal pollen with low abundances in the dataset will have been transported by wind from adjacent regions to the south and east. Generally, these pollen assemblages represent well the plant components in the alpine meadow communities, although they are influenced slightly by long-distance pollen transported by wind ~~or rivers (such as the arboreal pollen taxa; (~~Figure 2).

Table 1 Summary statistics for parameters in the pollen dataset. Min.: minimum; Med.: median; Max.: maximum. Units for ~~Longitude~~longitude and ~~Latitude~~latitude are ~~degree, for Altitude~~degrees, elevation is in m ~~a.s.l., for~~above sea level, Mt_{co}, Mt_{wa} and T_{ann} are °C, ~~for~~ P_{ann} is mm, ~~while for~~and pollen ~~daxa~~data are %.

Parameter	Min.	Med.	Max.	Mean
Longitude	91.80	97.20	99.79	96.42
Latitude	31.59	34.02	35.52	33.74
Elevation	3717	4422	5168	4399
Mt_{co}	-19.21	-15.61	-7.41	-15.09
Mt_{wa}	3.71	6.90	11.41	7.15
T_{ann}	-7.27	-3.72	2.27	-3.39
P_{ann}	226	491	689	471

Pollen taxa	Min.	Med.	Max.	Mean
Abies	0.00	0.00	0.38	0.01
Cedrus	0.00	0.00	0.19	0.00
Picea	0.00	0.00	2.52	0.10
Pinus	0.00	0.18	1.76	0.32
Alnus	0.00	0.00	0.67	0.11
Betula	0.00	0.00	0.94	0.11
Carpinus	0.00	0.00	0.63	0.06
Castanea	0.00	0.00	2.44	0.06
Corylus	0.00	0.00	1.88	0.07
Juglans	0.00	0.00	0.82	0.01
Oleaceae	0.00	0.00	0.16	0.00
Quercus	0.00	0.00	2.00	0.06
Salix	0.00	0.18	5.35	0.45
Ulmus	0.00	0.00	0.16	0.00
Chenopodiaceae	0.00	0.48	15.44	0.86
Ephedra	0.00	0.00	1.66	0.12
Ericaceae	0.00	0.00	0.19	0.01
Euphorbiaceae	0.00	0.00	0.19	0.00
Fabaceae	0.00	0.16	3.07	0.28
Hippophaë	0.00	0.00	5.62	0.27
Rhamnaceae	0.00	0.00	0.17	0.00
Ilex	0.00	0.00	0.18	0.00
Nitraria	0.00	0.00	0.51	0.01
Rosaceae	0.00	0.76	12.74	1.15
Tamaricaceae	0.00	0.00	0.75	0.03
Apiaceae	0.00	0.16	3.98	0.32
Artemisia	0.19	2.43	24.51	3.68
Asteraceae	0.00	1.46	33.56	2.09
Brassicaceae	0.00	0.36	28.17	1.22
Caryophyllaceae	0.00	0.16	2.26	0.23
Cyperaceae	4.84	76.24	95.91	68.67
Balsaminaceae	0.00	0.00	0.14	0.00
Urticaceae	0.00	0.00	3.87	0.08
Gentianaceae	0.00	0.16	4.85	0.40
Lamiaceae	0.00	0.00	1.05	0.12
Liliaceae	0.00	0.00	0.50	0.04
Plantaginaceae	0.00	0.00	0.88	0.03
Onagraceae	0.00	0.00	0.34	0.00
Papaveraceae	0.00	0.00	0.82	0.03
Poaceae	0.39	4.90	87.74	10.28
Polemoniaceae	0.00	0.00	15.21	0.34
Polygonum	0.00	0.49	20.50	1.47
Rumex	0.00	0.00	1.64	0.03
Koenigia	0.00	0.00	2.96	0.39
Primulaceae	0.00	0.00	0.56	0.03
Ranunculaceae	0.00	3.47	33.62	4.88
Saxifragaceae	0.00	0.00	4.69	0.10
Scrophulariaceae	0.00	0.00	0.71	0.01
Solanaceae	0.00	0.00	0.69	0.01
Thalictrum	0.00	0.98	12.05	1.45

The region covered by these modern pollen samples has a P_{ann} gradient from 226 to 689 mm, and cold thermal conditions with low T_{ann} ~~(-~~(−7.3 to 2.3 °C) and Mt_{co} ~~(-~~(−19.2 to ~~-~~−7.4 °C). A series of RDAs reveals that, relative to Mt_{co} and Mt_{wa}, P_{ann} explains more pollen assemblage variation (10.8% as a sole predictor in RDA) in the dataset (Table 2). A biplot of the RDA shows that the direction of the P_{ann} vector has a smaller angle with the positive direction of ~~Axis~~axis 1 (captures 43.2% of total inertia in the dataset) than with the positive direction of ~~Axis~~axis 2 (10.3%), indicating that the major component of ~~Axis~~axis 1 should be moisture. ~~The~~ RDA ~~separates~~ axis 1, which is highly correlated with P_{ann}, divides the pollen taxa into two groups generally~~,~~: Cyperaceae, Ranunculaceae, Rosaceae, and *Salix* indicating wet climatic conditions~~,~~ (located along the positive direction of P_{ann}), while Poaceae, *Artemisia*, and Chenopodiaceae represent drought (located along the negative direction of P_{ann}; Figure 3). ~~Since the~~Axis 2 is highly correlated with the two temperature variables; however these dominant pollen taxa have insignificant distributions along the axis, hence temperature is the secondary climatic variable for the pollen dataset relative to precipitation (Figure 3). Because of low occurrences and abundances for some rare pollen taxa, BRT models are only performed ~~successfully~~ for ~~only~~ 14 dominant or common pollen taxa. BRT modelling results ~~also~~ suggest that P_{ann} is the main climatic determinant for 9 out of 10 of the major pollen taxa with >0.6 prevalence, ~~while~~with Asteraceae ~~is a~~an exception ~~with~~having Mt_{co} as its main climatic determinant (68%; Table 3). BRT results reveal that pollen abundances of Cyperaceae, Ranunculaceae, and *Salix* are positively ~~relative~~related to P_{ann}, while those of Poaceae, *Artemisia*, and Chenopodiaceae have a negative relationship with P_{ann}, ~~which are~~ consistent with the RDA results (Figure 3 and 4; Appendix 1).

5 Potential use of the modern pollen dataset

~~Numerial~~Numerical analyses reveal that P_{ann} is the most important climatic determinant of pollen distribution in the eastern Tibetan Plateau, hence, P_{ann} is selected as the target variable in the calibration-set to assess the predictive power of this pollen dataset. Both approaches (WA-PLS, RF) perform well with low RMSEP values (the root mean square error of prediction) and high r^2 values (coefficient of determination between observed and predicted climatic variables; Figure 5). However, the plots of observed vs. predicted P_{ann} show a overestimate of P_{ann} for arid sites and an underestimate for wet sites (Figure 5). Hence, the inevitable “edge effects” should be treated with caution. Nevertheless, ~~the reconstruction with~~reconstructions covering ca. 400–500 mm P_{ann} should be reliable because of the low bias in the central part of the P_{ann} gradient (Figure 5).

Although the model performance of RF is not any better than that of WA-PLS, the reconstruction produced by RF might be more reliable as suggested by the statistical significance testing and comparison with modern observed P_{ann} for the two lakes (Koucha Lake and Xingxinghai Lake). Statistical significance testing ~~reveals~~shows that ~~reconstructions based on~~ the proportion of variance in the fossil data explained by the WA-PLS ~~explain~~reconstruction is less ~~proportion~~ than the 95% quantile of the ~~proportion of~~ variance explained by a reconstruction based on random environmental variables (999 ~~times~~trials) for the two lakes, while reconstructions ~~producted~~produced by RF explain a higher proportion ~~than the 95% quantile~~ (Figure 6). In other words, reconstructions produced by RF might be controlled by the major pollen components, because the explained proportion of variance in the fossil pollen spectra is closer to that explained by the first PCA axis, while reconstructions by WA-PLS could be influenced more by the pollen taxa with low abundances (Figure 6). The hypothesis that WA-PLS is ~~more~~ influenced more by low-abundance pollen taxa is supported by the high~~-~~variation in reconstructed P_{ann} among the fossil pollen samples (Figure 7). Relative to reconstructions of WA-PLS, results of RF have lower temporal variation and fewer outliers, and the predicted P_{ann} by RF is closer to the observed P_{ann} for the two lakes (Koucha Lake, 500 mm; Xingxinghai Lake, 350 mm) than that by WA-PLS.

Table 2 Summary statistics of redundancy analysis (RDA) of 19 pollen species and four climatic variables. VIF: variance inflation factor; P_{ann}: mean annual precipitation (mm); Mt_{co}: mean temperature of the coldest month (°C); Mt_{wa}: mean temperature of the warmest month (°C); T_{ann}: annual mean temperature (°C).

Climatic variables	VIF (without T_{ann})	VIF (with T_{ann})	Climatic variables as sole predictor	Marginal contribution based on climatic variables	
			Explained variance (%)	Explained variance (%)	*p*-value
P_{ann}	1.6	2.9	10.8	14.7	0.001
Mt_{co}	4.8	161.4	2.6	4.8	0.001
Mt_{wa}	3.8	83.9	1.6	1.3	0.100
T_{ann}	-	447.8	-	-	-

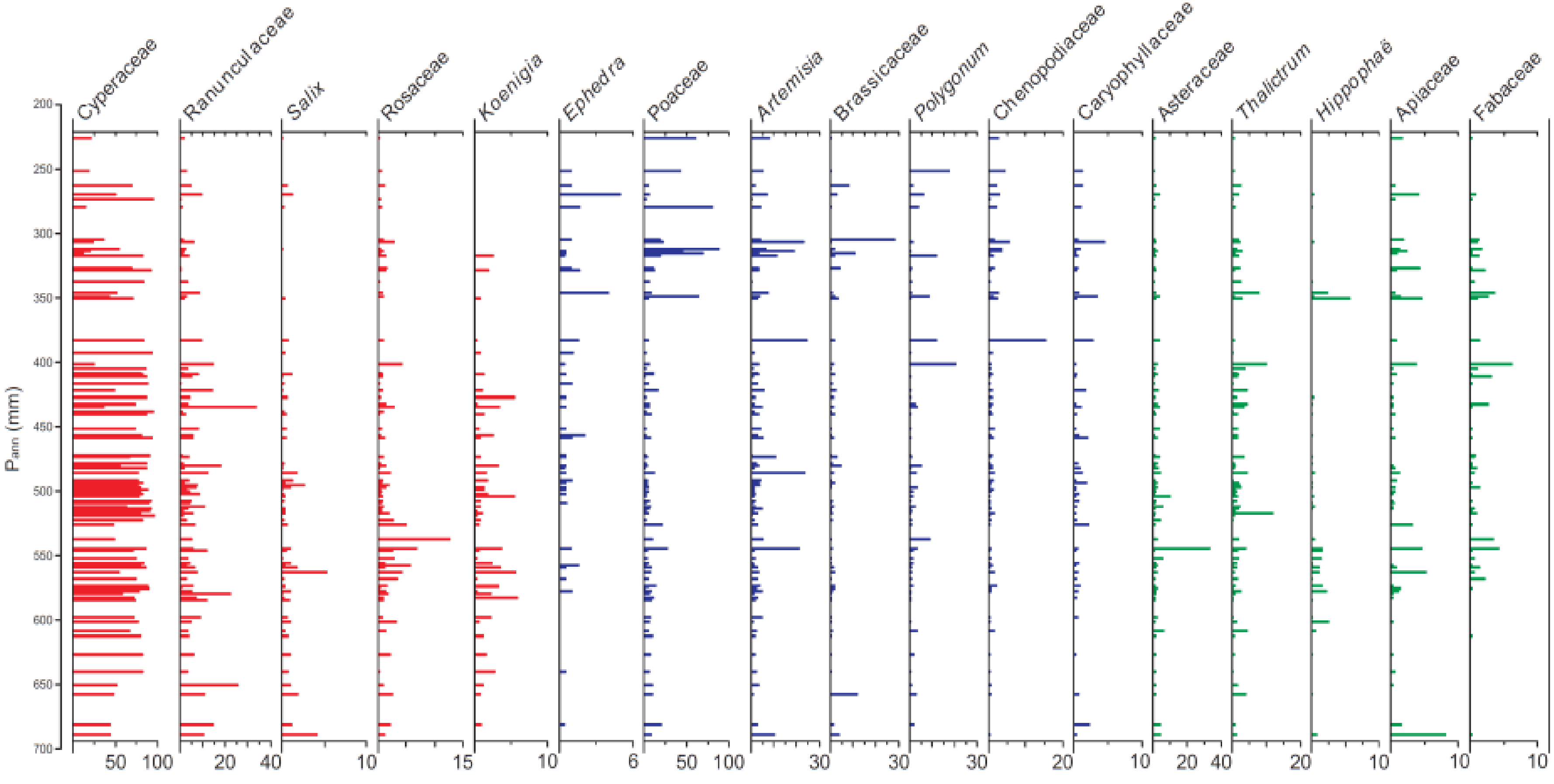

Figure 2 Pollen diagram showing the major taxa (percentage; %) of the 117 samples arranged by mean annual precipitation (P_{ann}; mm). Pollen taxa with red bars are positively related to P_{ann}, those with blue bars are negatively related to Pann, while the relationship is insignificant for those with green bars.

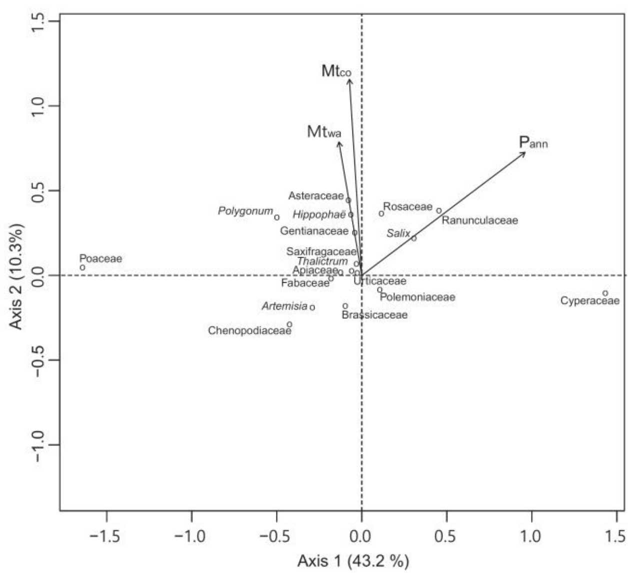

Figure 3 Plot of the first two redundancy analysis (RDA) axes showing the relationships between 18 pollen taxa (circles) and 3 climatic variables (arrows). P_{ann}: mean annual precipitation (mm); Mt_{co}: mean temperature of the coldest month (°C); Mt_{wa}: mean temperature of the warmest month (°C).

Table 3 Relative influence of climatic variables to the spatial distributions of 14 pollen taxa based on boosted regression tree (BRT) models. For each variable, the relative influence is expressed as a percentage among the three variables. Pollen taxa are ordered by decreasing prevalence (the proportion of sites in which each taxon is present).

Taxa	Prevalence	P_{ann}	Mt_{co}	Mt_{wa}
Cyperaceae	1.00	89.3%	7.5%	3.2%
Poaceae	1.00	95.1%	3.3%	1.5%
Artemisia	1.00	69.3%	12.9%	17.8%
Ranunculaceae	0.99	56.9%	33.7%	9.4%
Asteraceae	0.97	7.2%	68.0%	24.8%
Rosaceae	0.90	32.2%	52.7%	15.1%
Chenopodiaceae	0.85	89.1%	5.8%	5.1%
Brassicaceae	0.81	49.6%	37.4%	13.0%
Polygonum	0.75	42.8%	31.9%	25.3%
Salix	0.63	71.2%	21.7%	7.1%
Fabaceae	0.54	79.3%	11.0%	9.6%
Gentianaceae	0.54	10.5%	63.1%	26.4%
Apiaceae	0.53	33.6%	30.5%	35.9%
Hippophaë	0.37	9.6%	77.6%	12.9%
Number of > 50% relative influence:		7	3	0

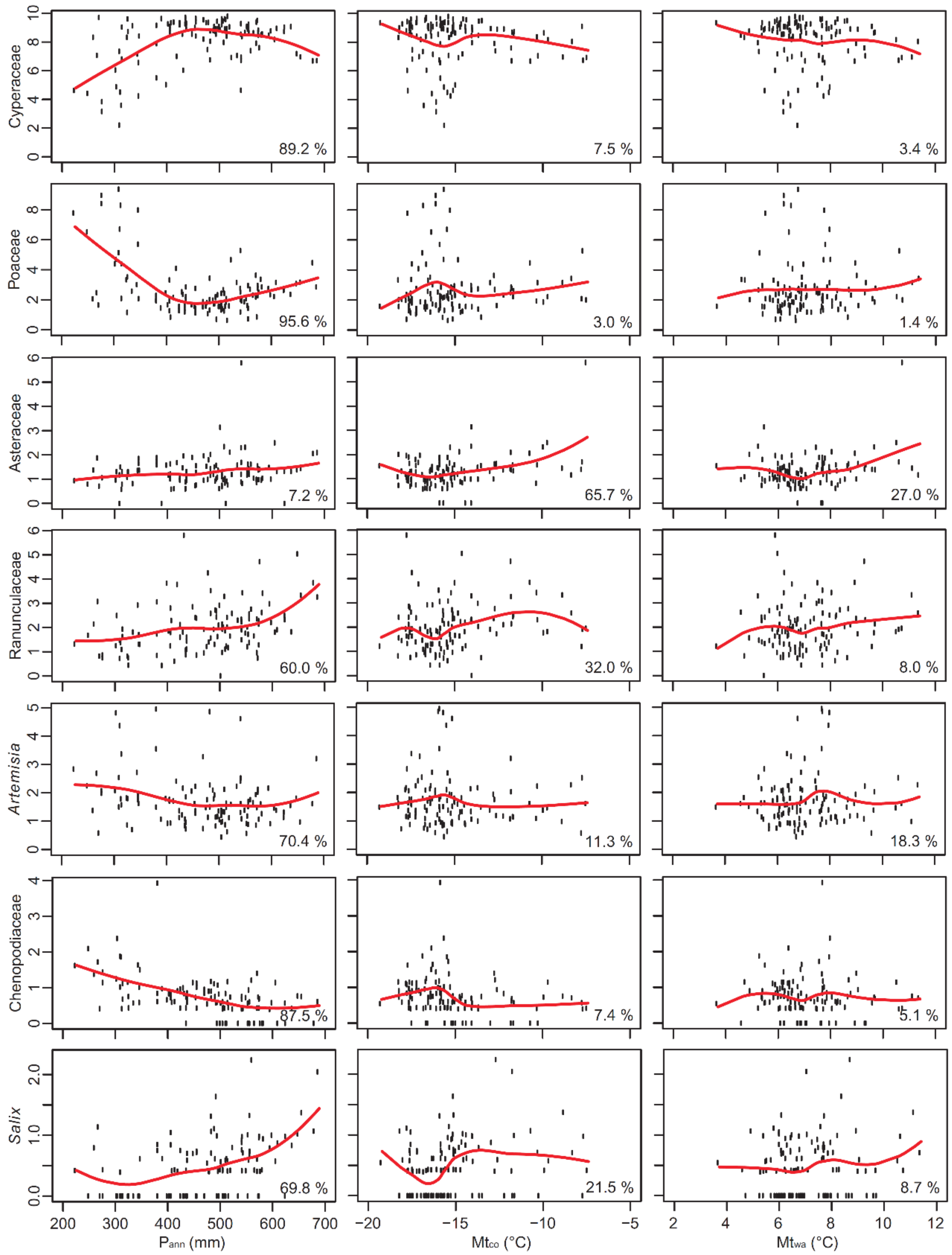

Figure 4 Boosted regression tree (BRT) modelled climate influences on pollen (seven dominant or major taxa) percentages. The pollen responses to three climatic variables (red curves) are fitted with local polynomial regression (LOESS).

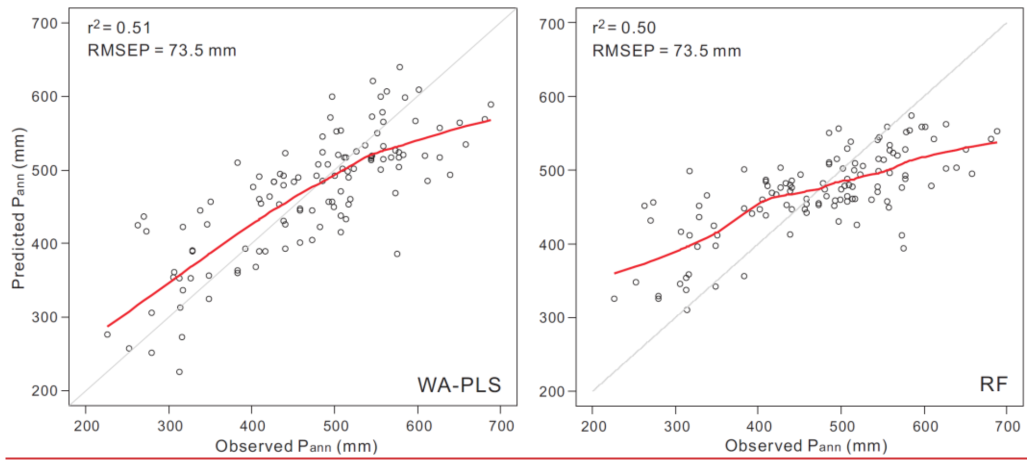

Figure 5 Scatter plots of observed annual precipitation (P_{ann}) vs. predicted P_{ann} by weighted averaging partial least squares regression (WA-PLS) and random forest algorithm (RF).

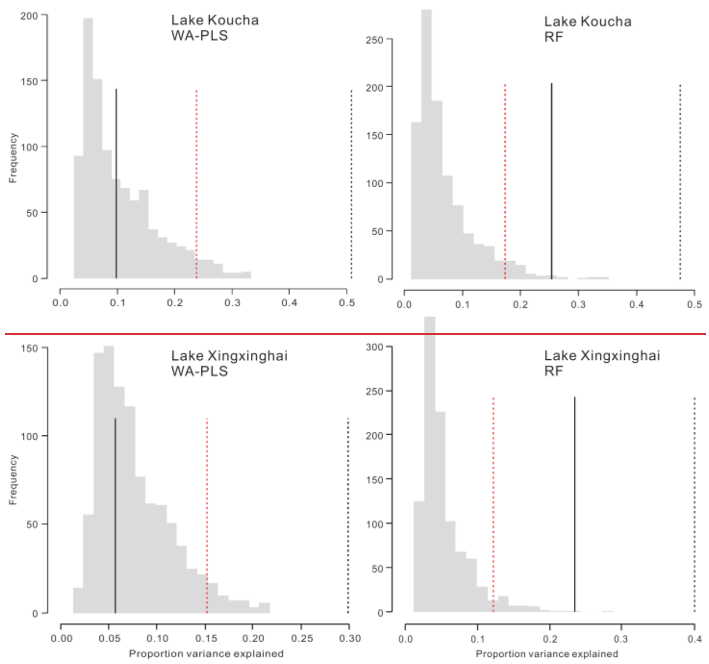

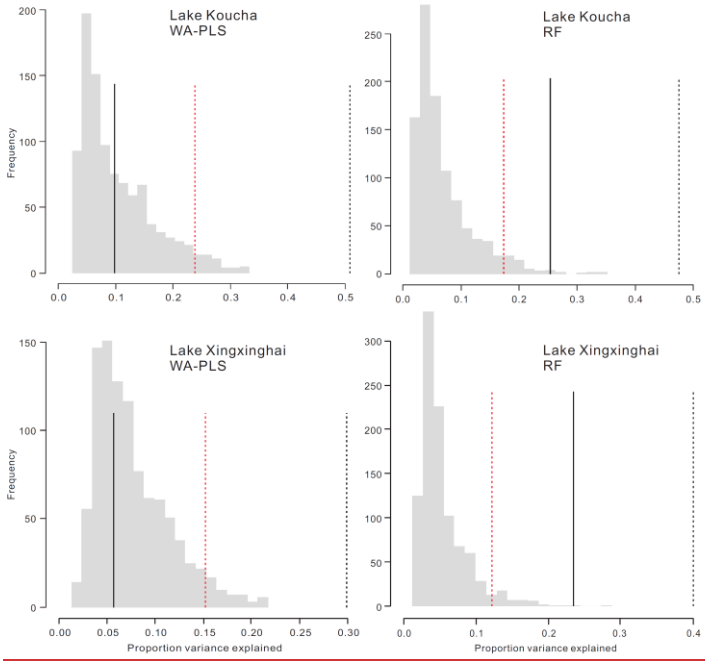

Figure 6 Statistical significance test of P_{ann} ~~reconstruction~~reconstructions from two lakes using weighted-averaging partial least squares regression (WA-PLS) and the random forest (RF) algorithm. Grey histograms indicate the proportion of variance in the fossil pollen spectra explained by random variables (999 times) and the red dotted line is the 95% quantile, the black dotted line is the variance in the pollen explained by the first PCA axis, and the black solid line is the explanation by the reconstructed P_{ann}.

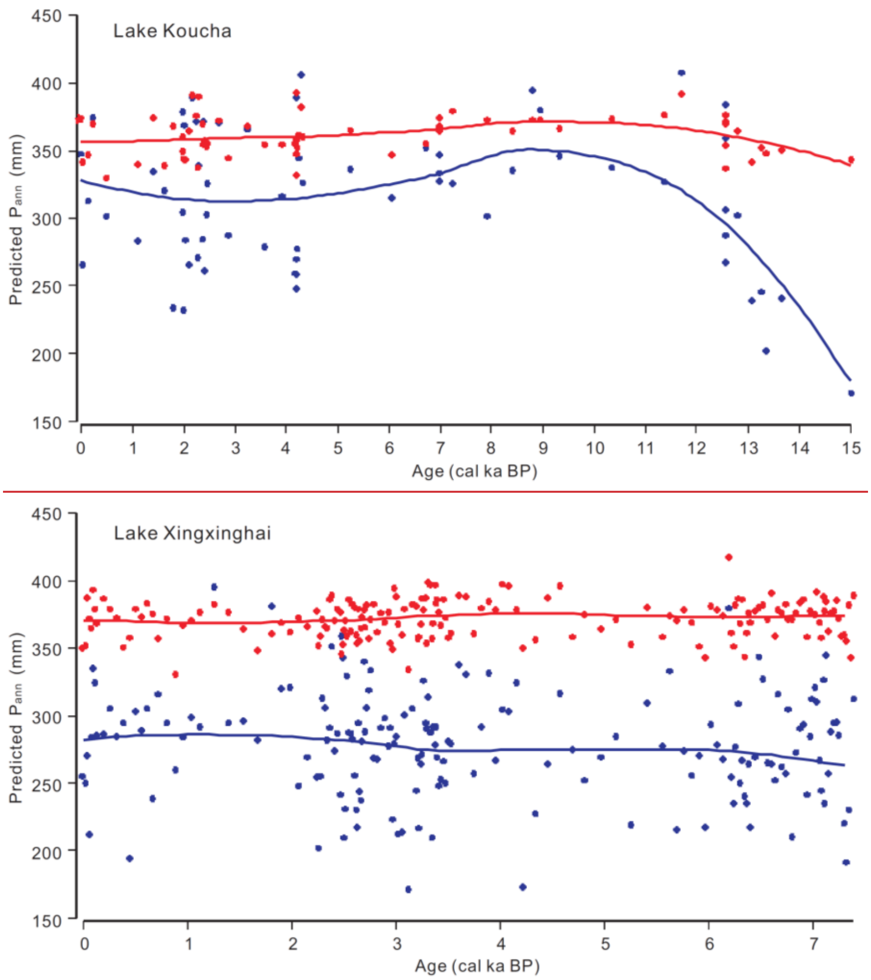
Lake Koucha
Predicted P ann (mm)
450
400
350
300
250
200
150
0 1 2 3 4 5 6 7 8 9 10 11 12 13 14 15
Age (cal ka BP)
Lake Xingxinghai
Predicted P ann (mm)
450
400
350
300
250
200
150
0 1 2 3 4 5 6 7
Age (cal ka BP)

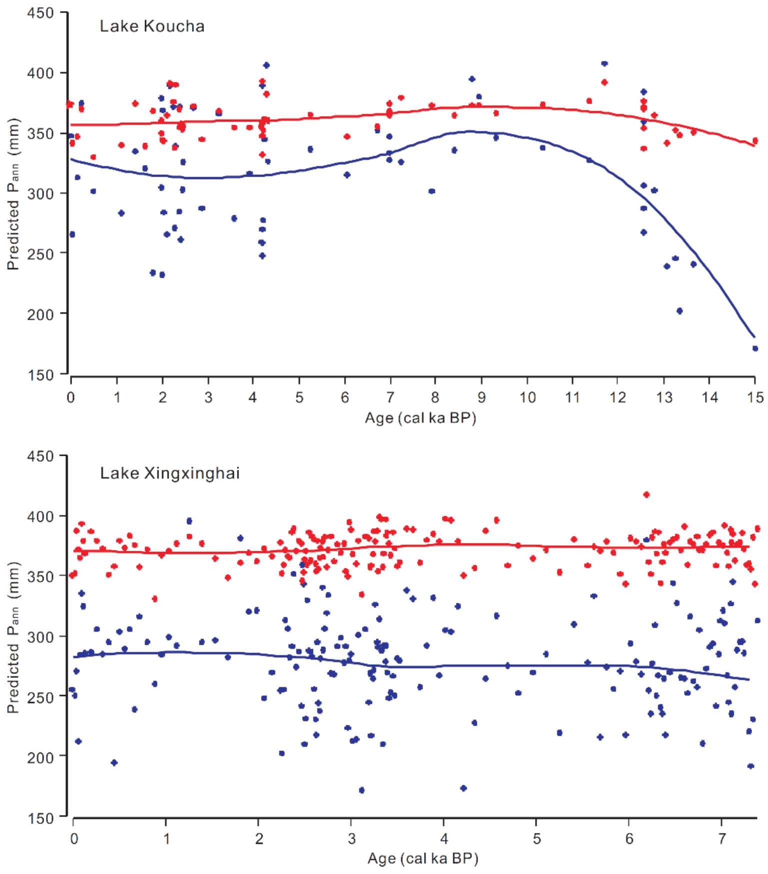

Figure 7 Annual precipitation (P_{ann}; mm) reconstructions for two Tibetan lakes using the weighted-averaging partial least squares regression (blue) and random forest algorithm (red). The curves are fitted by local polynomial regression (LOESS).

46 Data availability

Pollen datasets including both pollen counts and percentages for each sample together with their locations and climatic data are available at the National Tibetan Plateau Data Center (TPDC; DOI: 10.11888/Paleoenv.tpdc.271191).

7 Summary

We present a regional modern pollen dataset extracted from lake surface-sediments from the alpine meadow vegetation type on the Tibetan Plateau (eastern Tibetan Plateau, 91.8°–99.8°E and 31.6°–35.5°N), including pollen counts and pollen percentages together with their positions and climatic data. Numerical analyses reveal that P_{ann} is the most important climatic determinant for pollen distribution in the dataset, and our dataset behaves reliably and has good predictive power for past moisture reconstruction, and the random forest algorithm is a potentially ~~robust~~reliable approach in pollen-based past environment reconstruction.

In addition, our open-access dataset can fill the ~~geographic~~geographical gap left by the two previous modern pollen datasets (lake surface-sediments; Shen et al., 2006; Herzschuh et al., 2010) on the eastern Tibetan Plateau. By combining our dataset here with the previous ones (e.g. Herzschuh et al., 2019), a comprehensive modern pollen dataset is created covering vegetation types from the alpine forest to alpine steppe on the Tibetan Plateau, and will greatly improve the reliability of past vegetation reconstructions and climate estimations.

~~5 Data availability~~

~~Pollen datasets including both pollen counts and percentages for each sample together with their locations and climatic data are available at the National Tibetan Plateau Data Center (TPDC; DOI: 10.11888/Paleoenv.tpdc.271191).~~

Author contributions. XC and JN designed the pollen dataset. XC and KL collected pollen samples. XY and FT compiled the pollen identification and counting. XC and FT performed numerical analyses and organized the manuscript, LL and NW prepared the figures. All authors discussed the results and contributed to the final paper.

Acknowledgements

The sample collection and research were supported by the National Natural Science Foundation of China (Grant No. 41877459 and 41930323), CAS Pioneer Hundred Talents Program (Xianyong Cao) and Pan-Third Pole Environment Study for a Green Silk Road of CAS Strategic Priority Research Program (XDA20090000).

References

Birks, H.J.B., Heiri, O., Seppä, H. and Bjune, A.E.: Strengths and weaknesses of quantitative climate reconstructions based on late-Quaternary biological proxies, Open Ecol. J., 3, 68–110, 2010.

Cao, X., Tian, F. and Ding, W.: Improving the quality of pollen-climate calibration-sets is the primary step for ensuring reliable climate reconstructions, Sci. Bull., 63, 1317–1318, 2018.

Cao, X., Tian, F., Li, K. and Ni, J.: Atlas of pollen and spores for common plants from the east Tibetan Plateau. National Tibetan Plateau Data Center, DOI: 10.11888/Paleoenv.tpdc.270735, 2020.

Cao, X.Y., Herzschuh, U., Telford, R.J. and Ni, J.: A modern pollen-climate dataset from China and Mongolia: assessing its potential for climate reconstruction, Rev. Palaeobot. Palynol., 211, 87–96, 2014.

Fægri, K. and Iversen, J.: Textbook of pollen analysis, Munksgaard, Copenhagen, 1975.

He, J., Yang, K., Tang, W., Lu, H., Qin, J., Chen, Y. and Li, X.: The first high-resolution meteorological forcing dataset for land process studies over China, Sci. Data, 7, 25, DOI: 10.1038/s41597-020-0369-y, 2020.

Herzschuh, U., Birks, H.J.B., Mischke, S., Zhang, C. and Böhner, J.: A modern pollen-climate calibration set based on lake sediments from the Tibetan Plateau and its application to a Late Quaternary pollen record from the Qilian Mountains, J. Biogeogr., 37, 752–766, 2010.

Herzschuh, U., Cao, X., Laepple, T., Dallmeyer, A., Telford, R., Ni, J., Chen, F., Kong, Z., Liu, G., Liu, K.-B., Liu, X., Stebich, M., Tang, L., Tian, F., Wang, Y., Wischnewski, J., Xu, Q., Yan, S., Yang, Z., Yu, G., Zhang, Y., Zhao, Y. and Zheng, Z.: Position and orientation of the westerly jet determined Holocene rainfall patterns in China, Nat. Commun., 10, 2376, 2019.

Herzschuh, U., Kramer, A., Mischke, S. and Zhang, C.: Quantitative climate and vegetation trends since the late glacial on the northeastern Tibetan Plateau deduced from Koucha Lake pollen spectra. ~~Quaternary Research,~~Quat. Res., 71, 162–171, 2009.

Hijmans, R.J., Phillips, S., Leathwick, J. and Elith, J.: Dismo: Species Distribution Modeling, version 1.0-12, available at: http://CRAN.R-project.org/package/dismo, 2015.

Hill, M.O. and Gauch, H.G.: Detrended correspondence analysis: an improved ordination technique, Vegetatio, 42, 41–58, 1980.

Juggins, S. and Birks, H.J.B.: Quantitative environmental reconstructions from biological data, in: Birks, H.J.B., Lotter, A.F., Juggins, S. and Smol, J.P. (eds.), Tracking environmental change using lake sediments~~, –~~ (vol. 5~~:~~): Data handling and numerical techniques, Springer, Dordrecht, 431–494, 2012.

Juggins, S.: Rioja: analysis of Quaternary Science Data version 0.7-3, available at: http://cran.r-project.org/web/packages/rioja/index.html, 2012.

Li, J.F., Xie, G., Yang, J., Ferguson, D.F., Liu, X.D., Liu, H. and Wang, Y.F.: Asian Summer Monsoon changes the pollen flow on the Tibetan Plateau, Earth-Sci. Rev~~,~~., 202, 103114, 2020.

Liaw, A.: randomForest: Breiman and Cutler's Random Forests for Classification and Regression, available at: https://cran.r-project.org/web/packages/randomForest/index.html, 2018.

Ma, Q., Zhu, L., Wang, J., Ju, J., Lü, X., Wang, Y., Guo, Y., Yang, R., Kasper, T., Haberzettl, T. and Tang, L.: *Artemisia*/Chenopodiaceae ratio from surface lake sediments on the central and western Tibetan Plateau and its application, Palaeogeogr. Palaeoclim. Palaeoecol., 479, 138–145, 2017.

Maher, L.J.: Statistics for microfossil concentration measurements employing ~~sanmples~~samples spiked with marker grains, Rev. Palaeobot. Palynol., 32, 153–191, 1981.

Nychka, D., Furrer, R., Paige, J. and Sain, S.: fields: Tools for spatial data, version 9.6.1, available at: https://cran.r-project.org/web/packages/fields/, 2019.

Oksanen, J., Blanchet, F.G., Friendly, M., Kindt, R., Legendre, P., McGlinn, D., Minchin, P.R., O'Hara, R.B., Simpson, G.L., Solymos, P., Stevens, M.H.H., Szoecs, E. and Wagner, H.: vegan: Community Ecology Package, version 2.5-4, available at: https://cran.r-project.org/web/packages/vegan/index.html, 2019.

Prentice, I.C.: Multidimensional scaling as a research tool in Quaternary palynology: a review of theory and methods, Rev. Palaeobot. Palynol., 31, 71–104, 1980.

R Core Team: R, A language and environment for statistical computing, R Foundation for Statistical Computing, Vienna, 2019.

Shen, C., Liu, K.B., Tang, L. and Overpeck, J.T.: Quantitative relationships between pollen rain and climate in the Tibetan Plateau. Rev. Palaeobot. Palynol., 140, 61–77, 2006.

Sugita, S.: A model of pollen source area for an entire lake surface. Quat. Res., 39, 369–244, 1993.

Tang, L., Mao, L., Shu, J., Li, C., Shen, C. and Zhou, Z.: Atlas of Quaternary pollen and spores in China, Science Press, Beijing, 2017.

ter Braak, C.J.F. and Prentice, I.C.: A theory of gradient analysis, Adv. Ecol. Res., 18, 271–317, 1988.

ter Braak, C.J.F. and Verdonschot, P.F.M.: Canonical correspondence analysis and related multivariate methods in aquatic ecology, Aquat. Sci., 57, 255–289, 1995.

Tian, F., Xu, Q., Li, Y., Cao, X., Wang, X. and Zhang, L.: Pollen assemblage characteristics of lakes in the monsoon fringe area of China. Chinese Sci. Bull., 53(21), 3354–3363, 2008.

Wang, B.: The Asian Monsoon, Springer, Chichester, 2006.

Wang, F.X., Qian, N.F., Zhang, Y.L. and Yang, H.Q.: Pollen Flora of China, Science Press, Beijing, 1995.

Wu, Z.Y.: The vegetation of China. Science Press, Beijing, 1995 (in Chinese).

Appendix A

Boosted regression tree (BRT) modelled climate influences on pollen (seven common or minor taxa) percentages. The pollen responses to three climatic ~~variableds~~variables (red curves) are fitted with a local polynomial regression (LOESS).

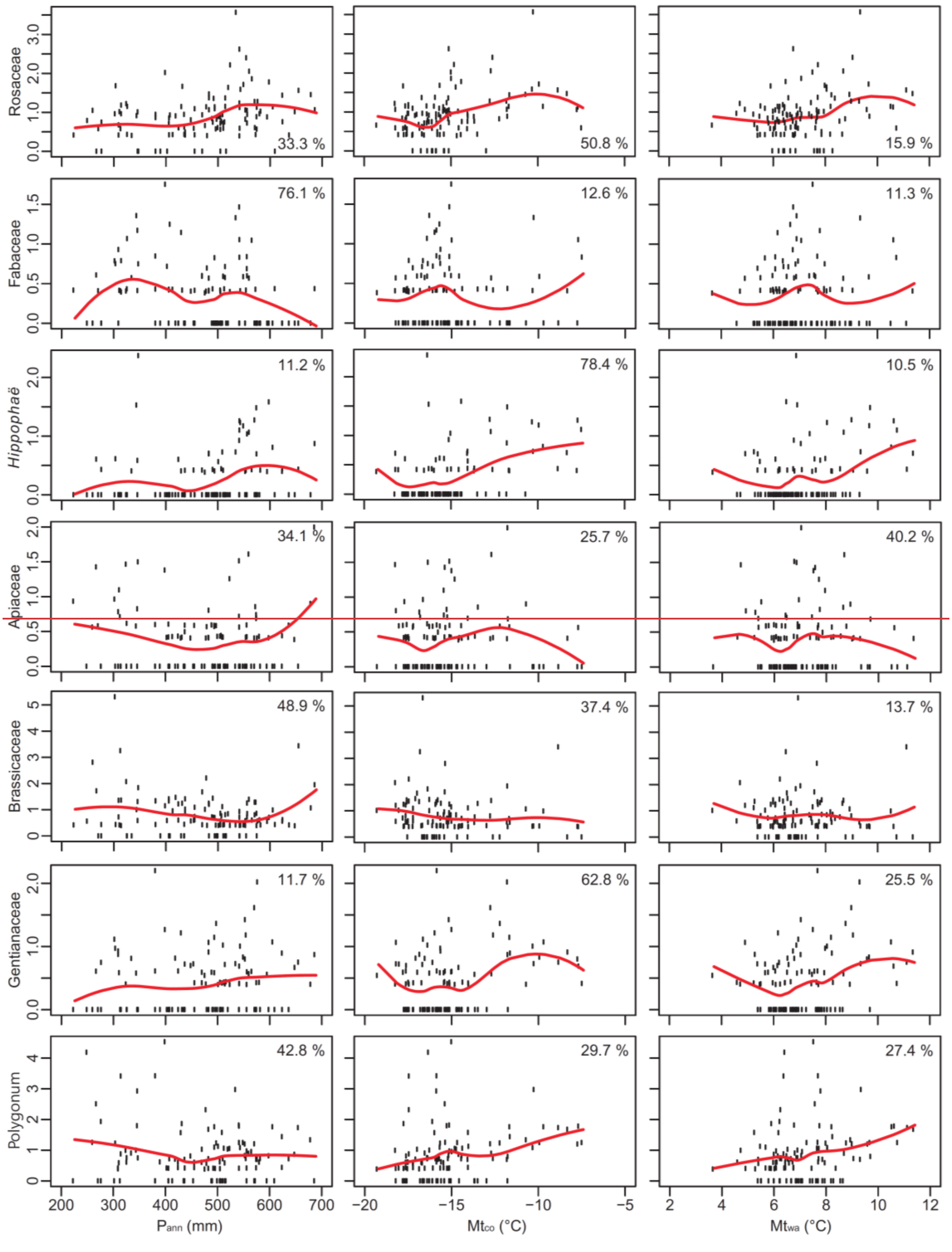
Rosaceae
33.3 %
50.8 %
15.9 %
Fabaceae
76.1 %
12.6 %
11.3 %
Hippophaë
11.2 %
78.4 %
10.5 %
Apiaceae
34.1 %
25.7 %
40.2 %
Brassicaceae
48.9 %
37.4 %
13.7 %
Gentianaceae
11.7 %
62.8 %
25.5 %
Polygonum
42.8 %
29.7 %
27.4 %
Pann (mm)
Mtco (°C)
Mtwa (°C)

423 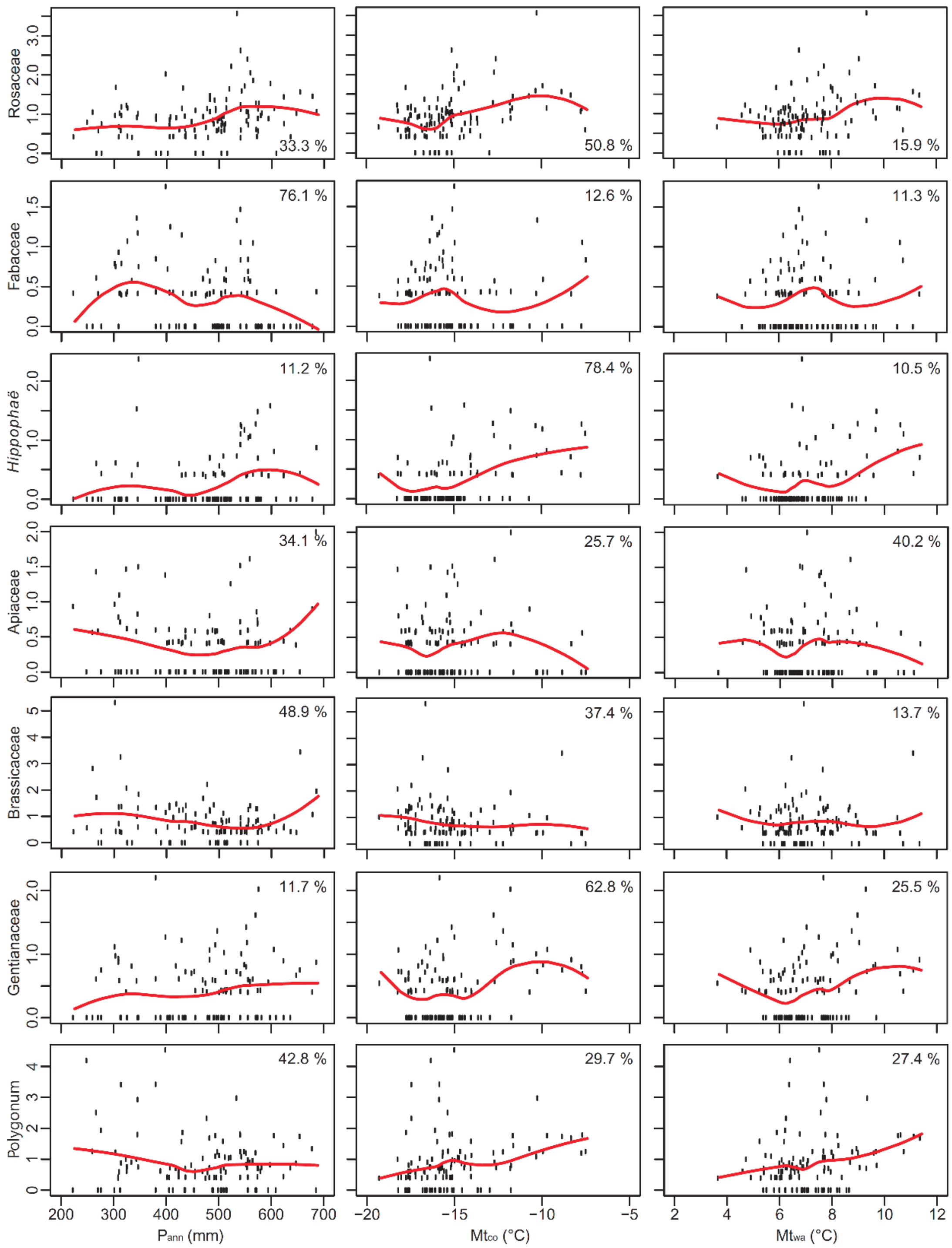
Rosaceae
Fabaceae
Hippophaë
Apiaceae
Brassicaceae
Gentianaceae
Polygonum
33.3 %
50.8 %
15.9 %
76.1 %
12.6 %
11.3 %
11.2 %
78.4 %
10.5 %
34.1 %
25.7 %
40.2 %
48.9 %
37.4 %
13.7 %
11.7 %
62.8 %
25.5 %
42.8 %
29.7 %
27.4 %
Pann (mm)
Mtco (°C)
Mtwa (°C)

424

Appendix B

Importance (imp) of pollen taxa on the spatial distribution of P_{ann} ~~were~~was repeatedly assessed by the random forest algorithm (RF). Shown in bold are the pollen taxa selected for the P_{ann} reconstruction based on RF.

Taxa	imp-run1	imp-run2	imp-run3	imp-run4	imp-run5
Abies	-1.5723				
Cedrus	0.0000				
Picea	0.3104	3.4397	3.5811	2.1705	1.1599
Pinus	-1.6225				
Alnus	-0.3501				
Betula	5.8217	7.4399	7.4490	5.7763	5.9524
Carpinus	-1.2049				
Castanea	-1.4692				
Corylus	0.2806	-0.3715			
Juglans	0.0000				
Oleaceae	0.0000				
Quercus	-0.4776				
Salix	9.2463	9.6372	10.0018	9.4944	10.2897
Ulmus	-0.6041				
Chenopodiaceae	17.7282	18.0369	16.8653	16.3110	18.5089
Ephedra	2.8306	2.9972	4.4539	3.5096	4.0226
Ericaceae	0.0755	1.7893	-0.2415		
Euphorbiaceae	-0.9748				
Fabaceae	2.4847	2.5302	3.5031	3.2985	1.8323
Hippophaë	5.5569	3.5027	4.0142	3.1174	4.5627
Rhamnaceae	0.0000				
Ilex	0.0000				
Nitraria	-1.0010				
Rosaceae	3.0053	4.8099	2.9771	3.6032	4.3940
Tamaricaceae	-2.3780				
Apiaceae	-0.6466				
Artemisia	1.7355	-0.0902			
Asteraceae	2.3902	1.7955	1.1307	-1.0880	
Brassicaceae	1.7269	2.2776	1.4596	1.5560	1.5308
Caryophyllaceae	-0.0033				
Cyperaceae	9.9824	9.8975	11.1838	10.4553	10.3560
Balsaminaceae	0.0000				
Urticaceae	0.8534	-1.4774			
Gentianaceae	1.1305	-0.8603			
Lamiaceae	3.3097	2.6853	3.4047	2.2080	2.6588
Liliaceae	-0.5353				
Plantaginaceae	2.3294	1.3210	1.4498	0.8906	0.8763

Onagraceae	1.0010	-0.8613			
Papaveraceae	0.1148	1.0344	-1.7028		
Poaceae	13.8815	14.5295	14.7793	15.7914	16.2655
Polemoniaceae	-0.5507				
Polygonum	0.0523	2.4552	2.9776	1.9432	2.3618
Rumex	1.0010	0.0000			
Koenigia	5.4498	4.3961	3.3305	4.1574	4.9186
Primulaceae	-1.2283				
Ranunculaceae	6.4799	8.9763	7.6140	7.5498	5.5157
Saxifragaceae	0.9422	1.3283	1.8760	4.1134	2.3728
Scrophulariaceae	-1.0010				
Solanaceae	1.0010	-1.0008			
Thalictrum	2.9345	2.3850	2.6363	2.4267	3.3457